Microcrystal electron diffraction-guided discovery of fungal metabolites

David A. Delgadillo,[a$] Lin Wu,[b$] Caroline Wang,[d] Yalong Zhang,[b] Jessica E. Burch,[a] Kunal K. Jha,[a] Lygia Silva de Moraes,[a] Gerald F. Bills,[e] Benjamin P. Tu,[d] Yi Tang,[b,c*] Hosea M. Nelson[a*]

[$] *Authors contributed equally.*

[a] *Division of Chemistry and Chemical Engineering, California Institute of Technology, Pasadena, CA 91125, United States.*

[b] *Departments of Chemical and Biomolecular Engineering,* [c] *Chemistry and Biochemistry, University of California, Los Angeles, Los Angeles, CA 90095, United States.*

[d] *Department of Biochemistry, University of Texas Southwestern Medical Center, Dallas, TX 75390, United States.*

[e] *Texas Therapeutic Institute, The Brown Foundation Institute of Molecular Medicine, University of Texas Health Science Center at Houston, Houston, TX 77054, United States.*

KEYWORDS: ArrayED, Electron Diffraction, MicroED, 3D ED, Natural Products, Metabolomics.

ABSTRACT: Nature remains a vast repository of complex and functional metabolites whose structural characterization continues to drive innovations in pharmaceuticals, agrochemicals, and materials science. The cryogenic electron microscopy (cryoEM) method, microcrystal electron diffraction (microED, a 3D ED technique) has emerged as a powerful tool to structurally characterize small molecules. Despite this emerging role in structural chemistry, the cost and throughput of microED have limited its application in the discovery of natural products (NPs). While recent advances in sample preparation (e.g. ArrayED) have provided a conceptual framework to address these challenges, they have remained unproven. Herein, we report the ArrayED-driven discovery of a structurally-unprecedented family of NPs (zopalide A-E), a muurolane-type sesquiterpene glycoside (rhytidoside A), aspergillicin analogs (aspergillicin H and aspergillicin I), and four crystal structures of previously reported fungal metabolites. We provide the first examples of absolute stereochemistry determination *via* microED for newly annotated NPs.

INTRODUCTION

From the seminal total synthesis of urea[1] to the discovery of penicillin as an antibiotic drug,[2] natural products (NPs) have played a critical role in biology, chemistry, and medicine. Indeed, NPs remain instrumental in modern medicine, comprising or inspiring over 50% of on-market drugs.[3] Despite this monumental societal impact, the discovery of structurally unique natural products has slowed over the last several decades.[4,5] While approximately 400,000 natural products have been discovered to-date, less than 1% of Earth's biodiversity has been investigated.[6] Many modern programs in NP discovery utilize a bioactivity-guided strategy, where fractionated NP extracts are subjected to biological assays and promising fractions are prioritized for further isolation, purification, and structural characterization.[7] Other strategies are structure-driven, where mass spectrometry (MS) or nuclear magnetic resonance (NMR) spectra collected from fractionated extracts are utilized to identify unannotated and potentially new NPs.[8,9] More recently, genome-mining approaches rely on bioinformatics to identify unique biosynthetic gene clusters that could lead to new NPs (Figure 1A).[10]

For bioactivity-, structure-, and genome mining-guided discovery campaigns, structural elucidation of nascent NPs

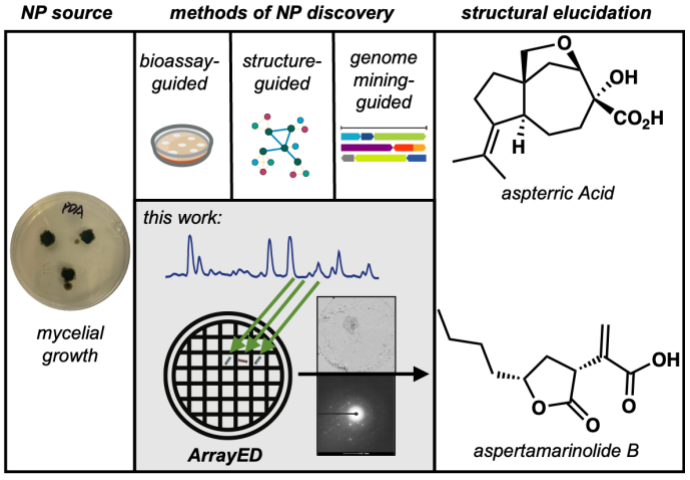

Figure 1. Approaches to NP discovery. Traditional methods of NP discovery that include bioassay-guided, structure-guided, and genome mining-guided isolation. In this work, we highlight the use of an electron diffraction-guided workflow (ArrayED) to discover NPs.

often limits throughput. Despite advances in modern analytical methods, combinations of NMR spectroscopy, MS, infrared (IR) spectroscopy, circular dichroism (CD), and ultraviolet-visible (UV-Vis) spectrophotometry data, are usually required to infer connectivity and atomic compositions, while *ab initio* determination of stereochemistry relies on single crystal X-ray diffraction (SCXRD). These methods often require milligram quantities of purified analyte and prior knowledge of the analyte.

MicroED, or 3D ED, has emerged as a complementary analytical approach that can address these limitations,[11–19] allowing for *ab initio* structural solutions from nanogram quantities of analyte and in some cases determination of absolute stereochemistry.[20,21] MicroED has been successfully implemented in traditional NP-discovery workflows, providing the structures of NPs identified in bioassay-,[22–24] structural-, [25,26] or bioinformatics-guided[27–33] approaches. However, it can take an hour or more to load and remove a single sample from a TEM, limiting throughput. With existing curated libraries of uncharacterized, bioactive NPs containing a million or more samples,[34,35] state-of-the-art microED is too expensive and too slow to address vast quantities of known unknowns in a meaningful way, let alone untapped NP space.

Our group recently reported the ArrayED workflow, where non-contact printing is used to deposit >100 of samples onto a single TEM grid, enabling high throughput (HT) screening for crystalline natural products amenable to microED (Figure 1B).[36] Herein, we report the application of ArrayED in a diffraction-guided NP discovery campaign, departing from bioassay-, structural- or genome mining-guided approaches. Our diffraction-guided approach is applied to the study of two fungal extracts, enabling the discovery of an unprecedented family of NPs zopalides A-E (**1**-**5**) (Figures 2 and 3) and a muurolane-type sesquiterpene glycoside rhytidoside A (**6**) (Figure 4), each having their absolute configuration established through dynamical refinement of microED data. Moreover, this workflow has enabled the full characterization of two new cyclic depsipeptide NPs: aspergillicin I (**7**), whose discovery would have proven challenging without a crystallographic model given the structural similarity to aspergillicin A, and aspergillicin H (**8**) (Figure 5). This screening strategy lays the groundwork for diffraction-guided NP discovery, which is poised to advance metabolomics and medicine.

RESULTS AND DISCUSSION

Initial efforts were focused on fungal strains TTI-0151 and TTI-0118 isolated from dead twigs and cow dung, respectively, during a field collection (Texas, USA). Morphological characteristics and rDNA sequence analysis identified TTI-0151 as *Rhytidhysteron hysterinum* and TTI-0118 as an undescribed *Zopfiella sp.* (see SI for details). The mycelial extracts of *R. hysterinum* and *Zopfiella sp.* were subjected to generalized HPLC to generate 96 time-resolved fractions. The microarray of each extract was then screened in a TEM for the presence of microcrystalline particles, those exhibiting diffraction were then binned as 'hits.'

Discovery of the Zopolide NP family derived from *Zopfiella sp.* ArrayED screening of 203 mg of extract isolated from the mycelial culture of *Zopfiella sp.* identified wells C7 and C9 as 'hits.' Deposition of these fractions onto individual grids revealed several crystals with high quality diffraction (Figure 2A) and allowed for collection of multiple continuous rotation datasets. The diffraction datasets were automatically

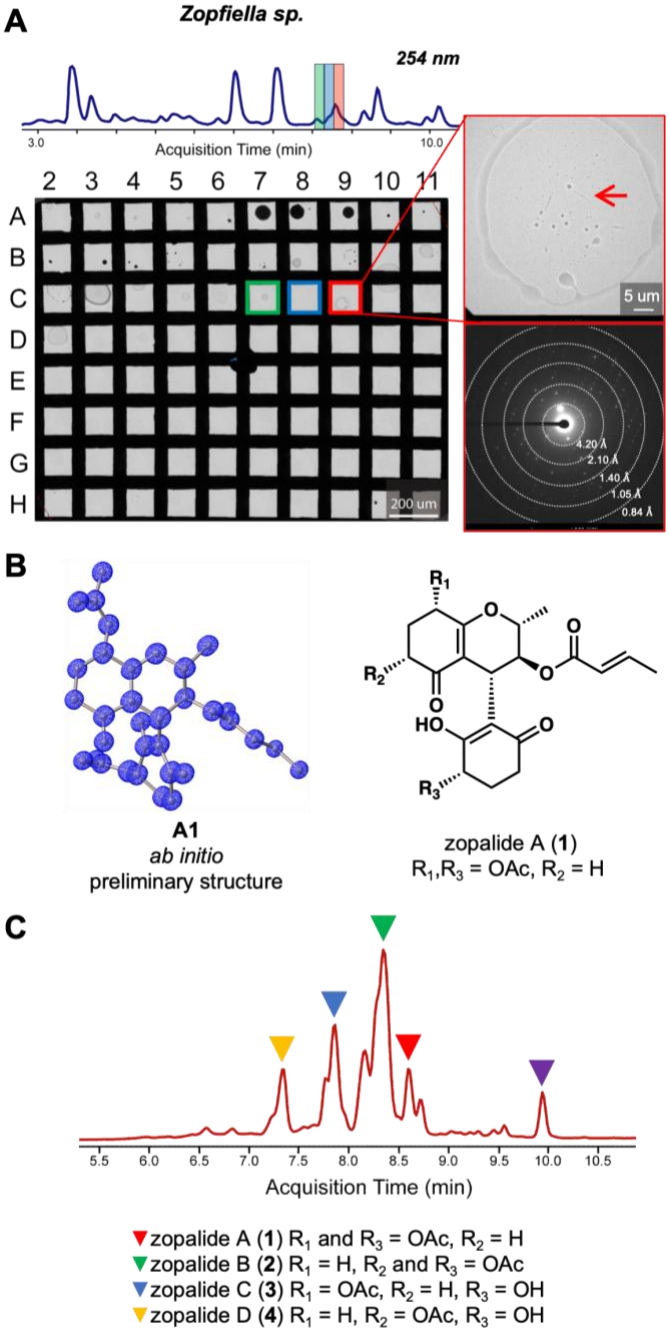

Figure 2. ArrayED screening overview for *Zopfiella sp.* and the discovery of Zopalide NPs. (A) Chromatogram of crude fungal extract of *Zopfiella sp.* at 254 nm wavelength with wells C7–C9 highlighted in green, blue, and red, respectively. Micrograph of the microarrayed extract with well C9 highlighted in red to show the presence of microcrystals and their associated diffraction pattern. (B) The *ab initio* preliminary solution **A1** (iso value = 1.085 eA^{-1}) that resulted from the screening of wells C7-C9 as well as the final structure of zopalide A (**1**). (C) Chromatogram from a HRMS experiment on well C7 of *Zopfiella sp.* marked to distinguish the corresponding structures.

processed with an in-house package *AutoProcess*.[37] Merging of three datasets from fraction C7 of *Zopfiella sp.* and *ab initio* phasing using kinematical approaches yielded scaffold **A1** (Figure 2B) in space group $P2_12_12_1$ (92.6% completeness at 0.8 Å resolution, $R_1$18.49%) (Figure S8). Initial similarity searches

for preliminary scaffold **A1** in public databases (Reaxys® and Dictionary of Natural Products) yielded no exact structural matches. To elucidate the molecular structure, we obtained high-resolution ESI-MS data to determine the molecular formula of scaffold **A1**, as similar scattering from C, N, and O at high resolution challenges *ab initio* compositional assignment with microED.[38]

Further HPLC-MS analysis of well C7 revealed a complex mixture of related congeners (Figure 2C). From well C7, we annotated five UV-active peaks corresponding to the following molecular formulas: $[C_{22}H_{26}O_9 + H]^+$, $[C_{22}H_{26}O_9 + H]^+$, $[C_{24}H_{28}O_{10} + H]^+$, $[C_{24}H_{28}O_{10} + H]^+$, and $[C_{22}H_{23}O_8 + H]^+$. We leveraged these data to assign the scaffold with atom identities and bond unsaturation to yield the proposed structure **1** (Figure 2B). Kinematic refinement in space group $P2_12_12_1$ provided high confidence of our assignment with 93.6% completeness at 0.8 Å resolution and R_1 14.92%. We named compound **1** as zopalide A (**1**).[39] Utilizing a modified dynamical refinement regime[21] structural models of both enantiomorphs were refined against the kinematic structure. The results suggested the absolute stereochemistry of zopalide A (**1**) as depicted in Figure 2B. A Z-score of 11.1σ obtained from the methods of Klarr and co-workers supports this assignment (Figure S10).[20]

Comparison of the refined structure of zopalide A (**1**) to public structural databases failed to yield an exact match. Given that this is the first NP to be characterized entirely by microED, we were compelled to validate this finding using traditional methods. A poor isolated yield (0.4 mg/L) of compound **1** from the mycelial extract required several rounds of scaled-up fermentation of *Zopfiella sp*. to obtain sufficient material for NMR confirmation (Table S1). The NMR data was consistent with the microED assignment.

With a scaled-up fermentation in hand, we pursued the structural characterization of the isomeric components identified earlier in HPLC-MS studies of well C7. Isomers **2**–**4** were isolated and characterized using traditional methods (HPLC-MS, NMR). Compound **2** was identified as a structural isomer of **1** and named zopalide B (Table S2)**.** Compounds **3** and **4** were named as zopalide C (**3**) and zopalide D (**4**) (Table S3 and S4) and are deacetylated analogs of metabolites **1** and **2** (Figure 2C). NMR spectra from a *m/z* 477 isomer appeared to have few analogous chemical shifts to spectra recorded from zopalides A-D (**1**–**4**) (Table S5). Microcrystals obtained by slow evaporation yielded the microED scaffold **B1** that would later be refined to reveal the structure of zopalide E (**5**) (Figure 3A).

Zopalide E (**5**) is proposed to be an intramolecular oxa-Michael addition product of zopalide B (**2**) (Scheme S1) representing the most structurally complex member of the Zopalide family. Various stereocenters in compound **5,** notably the stereocenter appending the acetylcyclohexanone to the fused ring system, were observed to be inverted relative to compound **2**. To elucidate the absolute configuration, we utilized a modified dynamical refinement approach[21] where structural models of both enantiomorphs of compound **5** were refined against the kinematic structures. Results of dynamical refinement (Figure 3B) suggested the absolute stereochemistry of zopalide E (**5**) as depicted in Figure 3A.

To further validate the ArrayED-driven discovery of these unprecedented natural products, a final round of fermentation, purification and isolation were undertaken to provide material for SCXRD, providing a structure consistent with the microED structure (Figure S12B). The root mean square deviation (RMSD) of the structural models provided by microED and SCXRD was 0.037 Å (Figure 3C), further supporting the consistency and reliability of microED data. Flack and Hooft parameters suggest that we have correctly assigned the absolute configuration of zopalide E (**5**) previously determined by dynamical refinement of microED data. Together, this family of NPs represents the first examples of molecular discovery using a diffraction-guided approach and the first application of dynamical refinement to establish the absolute configuration of newly discovered NP. Moreover, it reinforces electron diffraction as a robust method for the structural elucidation of novel natural products without structural precedent.

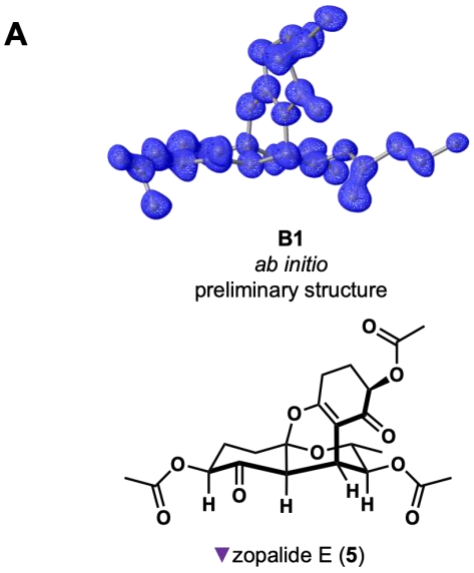

B

	zopalide E (**5**) enant2	enant1
R_1	0.1225	0.1476
wR_2	0.1332	0.1531
Z-score	14.6σ	

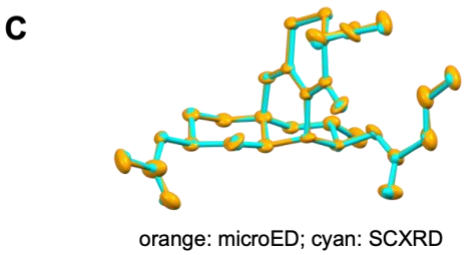

Figure 3. Reisolation from *Zopfiella sp.* and the discovery of zopalide analogs. (A) *ab initio* preliminary solution **B1** (iso value = 0.772 eA^{-1}) in space group C_2 provided by microED data collection on the final analyte isolated from the Zopalide family, followed by the final structure of zopalide E (**5**). (B) Statistics calculated from the dynamical refinement of both enantiomorphs of compound **5** in space group $P2_12_12_1$. (C) Superposition of the structure provided by microED in space group $P2_12_12_1$ and the structure provided by SCXRD in space group $P2_12_12_1$ with an RSMD of 0.037 Å.

Discovery of muurolane-type sesquiterpene glycoside derived from *Rhytidhysteron hysterinum*. With this success, we applied ArrayED screening to 88 mg of crude extract isolated from the mycelium of *Rhytidhysteron hysterinum*. We observed crystalline particles in 24 of the 96 microarrayed fractions (Figure 4A). Deposition of the best diffracting particles, obtained from well D8, onto a TEM grid yielded several continuous rotation datasets. Merging two of the highest quality datasets yielded preliminary scaffold C**1** (Figure 4B) in space group $P2_1$ with 87.2% completeness at 1.0 Å resolution (R_1 34.08%). A structural database search returned several sub-structure matches to muurolane-type sesquiterpene glycosides, but no exact matches. HPLC-MS analysis of well D8 revealed a heterogeneous mixture containing at least seven detectable analytes (Figure S15, i).

We later matched our preliminary solution to the *m/z* 407.2305 $[M + Na]^+$ peak. Following bond length and bond angle analysis, refinement of **C1** to space group $P2_1$ revealed a new NP which we have named rhytidoside A (**6**) (86.4% completeness, 0.8 Å , R_1 13.06%) (Figure 3B). Dynamical refinement established the absolute stereochemistry of rhytidoside A (**6**) as shown with a Z-score of 2.8σ (Figure S16). Notably, comparison of the refined structure **6** against published muurolane-type sesquiterpene glycodsides revealed structural similarities with the balanoindicosides isolated from the plant *Balanophora fungosa* subspecies *Indica*.[40]

Isolation and Characterization of *Rhytidhysteron hysterinum* derived metabolites. Encouraged by the discovery of rhytidoside A (**6**) we set out to isolate and characterize more NPs from this strain, as several diffracting fractions were identified during initial ArrayED screening (highlighted wells in Figure 3A). In addition to rhytidoside A (**6**), two unrelated new secondary metabolites were discovered, aspergillicin H (**7**) and aspergillicin I (**8**). Moreover, within this extract, microED structures of previously reported aspergillicin A (**9**), aspergillicin F (**10**),[41] cyclopiazonic acid (**11**),[42] aspertamarinolide B (**12**),[43,44] and aspertamarinolide D (**13**)[45] were determined (Figure 5). All the isolated metabolites in Figure 5, aside from **8,** yielded microED structures and were subsequently validated through HPLC-MS and NMR (Tables S6-S11). Compounds **12** and **13** were co-isolated and characterized in co-crystal form (Figure S17).

SUMMARY

Utilization of the ArrayED screening workflow enabled the discovery of nine previously undescribed NPs (compounds **1-8**) and the first crystal structure of four previously reported NPs (compounds **9-13**). It is notable that accurately annotating the structure of cyclic peptides such as aspergillicin A and aspergillicin I, where the relative positions of the valine and isoleucine are interchanged, would be intractable using state-of-the-art structural elucidation methodology. Moreover, absolute stereochemistry of several of these NPs was determined using dynamical refinement on microED data. This work exemplifies how electron diffraction can be used to direct NP isolation and discovery unbiased by biosynthetic origin, structure, polarity, or activity. Given that several new NPs were discovered with as little as 88 milligrams of extract, this study paves the way for a powerful application of diffraction science in NP discovery. Efforts are currently underway to synthesize and evaluate the bioactivity of these NPs.

ASSOCIATED CONTENT

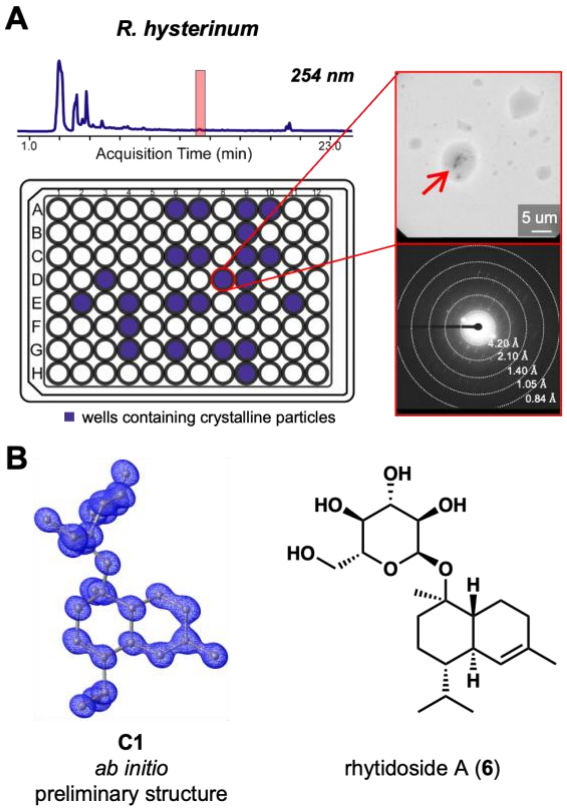

Figure 4. ArrayED screening overview of *Rhytidhysteron hysterinum*. (A) Chromatogram of mycelial extract from *Zopfiella sp.* at 254 nm wavelength with fraction D8 highlighted in red. Depiction of the 96 fractions generated for the ArrayED workflow with wells containing crystalline particles highlighted in violet. Particles from well D8 are shown along with the corresponding diffraction. (B) *ab initio* preliminary solution **C1** (iso value = 0.44 eA^{-1}) that resulted from the screening of well D8 (duplicate molecules found in the assymetric unit omitted for clarity), followed by the final structure of rhytidoside A (**6**).

Data Availability Statement

The raw MicroED data for this study are available on Zenodo. The autoprocessing python script utilized in this study is available at GitHub. CCDC xxxxxx–xxxxxx contains the supplementary crystallographic data for this paper. These data can be obtained free of charge via www.ccdc.cam.ac.uk/data_request/cif, or by emailing data_request@ccdc.ac.uk, or by contacting The Cambridge Crystallographic Data Centre, 12 Union Road, Cambride CB2 1EZ, UK; fax + 44 1223 336033.

Supporting Information

The Supporting Information is available free of charge on the ACS Publications website.

Detailed experimental protocols on sample preparation of fungal culture, extraction procedure, 96-well fractionation scheme, and compound isolation procedure; supporting data for ArrayED screening, structural models, and NMR characterization; preliminary solutions and fully refined structural solutions for identified crystalline natural products. (PDF)

AUTHOR INFORMATION

Corresponding Authors

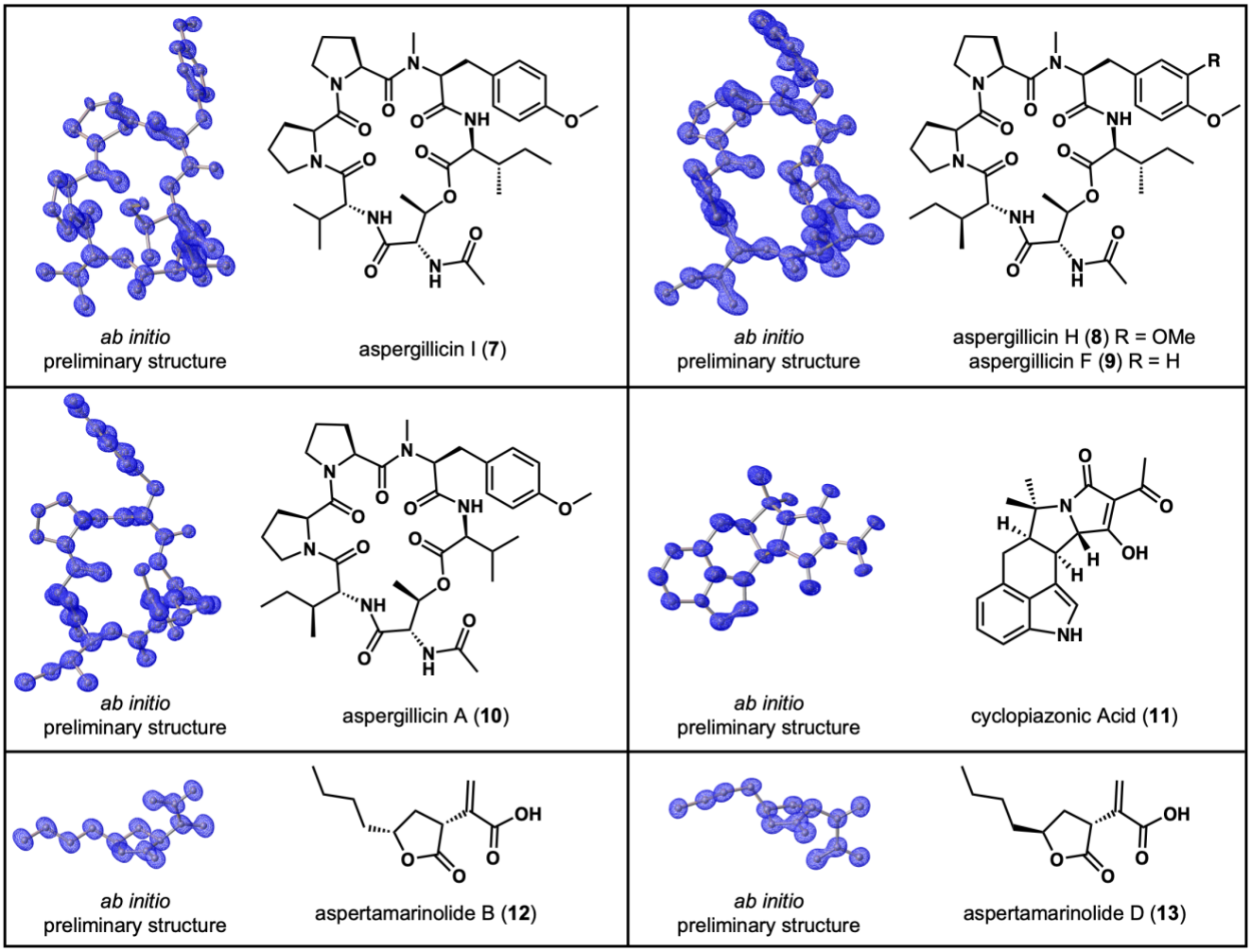

Figure 5. MicroED structures of fungal metabolites identified from the mycelial extract of *R. hysterinum*. Depictions of the *ab inito* solution of compound **7** (iso value = 0.556 eA^{-1}), compound **9** (iso value =1.4 eA^{-1}), compound **10** (iso value = 0.648 eA^{-1}), compound **11** (iso value = 0.955 eA^{-1}), compound **12** (iso value = 0.592 eA^{-1}), and compound **13** (0.571 eA^{-1}).

*Hosea M. Nelson – *Division of Chemistry and Chemical Engineering, California Institute of Technology, Pasadena, CA 91125, United States.*
Email: hosea@caltech.edu

*Yi Tang – Departments of Chemical and Biomolecular Engineering and Department of Chemistry and Biochemistry, University of California, Los Angeles, Los Angeles, CA 90095, United States.
Email: yitang@g.ucla.edu

Authors

David A. Delgadillo – *Division of Chemistry and Chemical Engineering, California Institute of Technology, Pasadena, CA 91125, United States.*

Lin Wu – *Departments of Chemical and Biomolecular Engineering, University of California, Los Angeles, Los Angeles, CA 90095, United States.*

Caroline Wang – *Department of Biochemistry, University of Texas Southwestern Medical Center, Dallas, TX 75390-9152, United States.*

Yalong Zhang – *Departments of Chemical and Biomolecular Engineering, University of California, Los Angeles, Los Angeles, CA 90095, United States*

Jessica E. Burch – *Division of Chemistry and Chemical Engineering, California Institute of Technology, Pasadena, CA 91125, United States.*

Kunal K. Jha – *Division of Chemistry and Chemical Engineering, California Institute of Technology, Pasadena, CA 91125, United States.*

Lygia Silva de Moraes – *Division of Chemistry and Chemical Engineering, California Institute of Technology, Pasadena, CA 91125, United States.*

Benjamin P. Tu – *Department of Biochemistry, University of Texas Southwestern Medical Center, Dallas, TX 75390-9152, United States.*

Author Contributions

DAD and HMN conceptualized the workflow and methodology. DAD collected data and carried out the workflow. LW and YT conducted the culturing and isolation experimentation. CW and BPT conducted the bioassay experimentation. JEB, KKJ, and LSM carried out structural refinement. HMN, YT, and BPT

supervised experimentation. DAD and HMN wrote the original manuscript draft and HMN, KKJ, LW, CW, YT, and BPT edited the manuscript.

Funding Sources

This research was funded by NIH NCCIH 1 R01AT011990 (H.M.N. and Y.T.), HHMI Emerging Pathogen Initiative, Packard Foundation (H.M.N.), and Pew Charitable Trust (H.M.N.).

Notes

The authors declare no competing financial interests.

ACKNOWLEDGMENT

We thank Dr. Songye Chen (Caltech) and the Caltech Cryo-EM facility for materials and advice, Dr. Scott Virgil (Caltech) for expertise with instrumentation, Donald W. Crocker for helpful discussions, the Resnick High Performance Computing Cluster (Caltech) for computational resources, and Dr. Michael Takase (Caltech) for assistance with X-ray crystallography.

ABBREVIATIONS

3D ED, three dimensional electron diffraction; CD, circular dichroism; cryoEM, cryogenic electron microscopy; HPLC, high performance liquid chromatography; HT, high throughput; IR, infrared; microED, microcrystalline electron diffraction; MS, mass spectrometry; NMR, nuclear magnetic resonance; NP(s), natural product(s); SCXRD, single crystal X-ray diffraction; UV-Vis, ultra violet-visible spectrometry

REFERENCES

(1) Wöhler, F. Ueber Künstliche Bildung Des Harnstoffs. *Ann. Phys.* **1828**, *87* (2), 253–256.

(2) Fleming, A. On the Antibacterial Action of Cultures of a Penicillium, with Special Reference to Their Use in the Isolation of B. Influenzae. *The British Journal of Experimental Pat.* **1929**, *10*, 226–236.

(3) Newman, D. J.; Cragg, G. M. Natural Products as Sources of New Drugs over the Nearly Four Decades from 01/1981 to 09/2019. *J. Nat. Prod.* **2020**, *83* (3), 770–803.

(4) Pye, C. R.; Bertin, M. J.; Lokey, R. S.; Gerwick, W. H.; Linington, R. G. Retrospective Analysis of Natural Products Provides Insights for Future Discovery Trends. *Proc. Natl. Acad. Sci. U. S. A.* **2017**, *114* (22), 5601–5606.

(5) Atanasov, A. G.; Zotchev, S. B.; Dirsch, V. M.; International Natural Product Sciences Taskforce; Supuran, C. T. Natural Products in Drug Discovery: Advances and Opportunities. *Nat. Rev. Drug Discov.* **2021**, *20* (3), 200–216.

(6) Harvey, A. L.; Edrada-Ebel, R.; Quinn, R. J. The Re-Emergence of Natural Products for Drug Discovery in the Genomics Era. *Nat. Rev. Drug Discov.* **2015**, *14* (2), 111–129.

(7) Wilson, B. A. P.; Thornburg, C. C.; Henrich, C. J.; Grkovic, T.; O'Keefe, B. R. Creating and Screening Natural Product Libraries. *Nat. Prod. Rep.* **2020**, *37* (7), 893–918.

(8) Vitale, G. A.; Geibel, C.; Minda, V.; Wang, M.; Aron, A. T.; Petras, D. Connecting Metabolome and Phenotype: Recent Advances in Functional Metabolomics Tools for the Identification of Bioactive Natural Products. *Nat. Prod. Rep.* **2024**, *41* (6), 885–904.

(9) Blue, R. M.; Macho, J. M.; Lee, H.-W.; MacMillan, J. B. 11B and 1H-11B HMBC NMR as a Tool for Identification of a Boron-Containing Nucleoside Dimer. *J. Nat. Prod.* **2022**, *85* (11), 2682–2686.

(10) Yee, D. A.; Niwa, K.; Perlatti, B.; Chen, M.; Li, Y.; Tang, Y. Genome Mining for Unknown-Unknown Natural Products. *Nat. Chem. Biol.* **2023**, *19* (5), 633–640.

(11) Jones, C. G.; Martynowycz, M. W.; Hattne, J.; Fulton, T. J.; Stoltz, B. M.; Rodriguez, J. A.; Nelson, H. M.; Gonen, T. The CryoEM Method MicroED as a Powerful Tool for Small Molecule Structure Determination. *ACS Cent. Sci.* **2018**, *4* (11), 1587–1592.

(12) Kunde, T.; Schmidt, B. M. Microcrystal Electron Diffraction (MicroED) for Small-Molecule Structure Determination. *Angew. Chem. Int. Ed Engl.* **2019**, *58* (3), 666–668.

(13) Bruhn, J.; Scapin, G.; Cheng, A.; Ganesh, T.; Dallakyan, S.; Read, B.; Nieusma, T.; Lucier, K.; Mayer, M.; Chiang, N.; Poweleit, N.; McGilvray, P.; Wilson, T.; Mashore, M.; Hennessy, C.; Thomson, S.; Potter, C.; Carragher, B. Small Molecule Microcrystal Electron Diffraction (MicroED) for the Pharmaceutical Industry – Results from Examining over Fifty Samples. *Microsc. Microanal.* **2021**, *27* (S1), 2594–2598.

(14) Martynowycz, M. W.; Gonen, T. Microcrystal Electron Diffraction of Small Molecules. *J. Vis. Exp.* **2021**, No. 169.

(15) Richards, L. S.; Flores, M. D.; Millán, C.; Glynn, C.; Zee, C.-T.; Sawaya, M. R.; Gallagher-Jones, M.; Borges, R. J.; Usón, I.; Rodriguez, J. A. Fragment-Based Ab Initio Phasing of Peptidic Nanocrystals by MicroED. *ACS Bio Med Chem Au* **2023**, *3* (2), 201–210.

(16) Lin, J.; Unge, J.; Gonen, T. Distinct Conformations of Mirabegron Determined by MicroED. *Adv. Sci. (Weinh.)* **2023**, *10* (34), e2304476.

(17) Bu, G.; Danelius, E.; Wieske, L. H. E.; Gonen, T. Polymorphic Structure Determination of the Macrocyclic Drug Paritaprevir by MicroED. *Adv. Biol. (Weinh.)* **2024**, *8* (5), e2300570.

(18) Ge, S.; Fu, M.; Gu, D.; Cai, Z.; Wei, L.; Yang, S.; Wang, H.; Ge, M.; Wang, Y. Comparing Microcrystal Electron Diffraction (MicroED) and X-Ray Crystallography as Methods for Structure Determination of Oseltamivir Phosphate. *J. Mol. Struct.* **2024**, *1308*, 138085.

(19) Lin, J.; Unge, J.; Gonen, T. Unraveling the Structure of Meclizine Dihydrochloride with MicroED. *Adv. Sci. (Weinh.)* **2024**, *11* (6), e2306435.

(20) Klar, P. B.; Krysiak, Y.; Xu, H.; Steciuk, G.; Cho, J.; Zou, X.; Palatinus, L. Accurate Structure Models and Absolute Configuration Determination Using Dynamical Effects in Continuous-Rotation 3D Electron Diffraction Data. *Nat. Chem.* **2023**, *15* (6), 848–855.

(21) de Moraes, L. S.; Burch, J. E.; Delgadillo, D. A.; Rodriguez, I. H.; Mai, H.; Smith, A. G.; Caille, S.; Walker, S. D.; Wurz, R. P.; Cee, V. J.; Rodriguez, J. A.; Gostovic, D.; Quasdorf, K.; Nelson, H. M. Structural Elucidation and Absolute Stereochemistry for Pharma Compounds Using MicroED. *Org. Lett.* **2024**, *26* (33), 6944–6949.

(22) Park, J.-D.; Li, Y.; Moon, K.; Han, E. J.; Lee, S. R.; Seyedsayamdost, M. R. Structural Elucidation of Cryptic Algaecides in Marine Algal-Bacterial Symbioses by NMR Spectroscopy and MicroED. *Angew. Chem. Int. Ed Engl.* **2022**, *61* (4), e202114022.

(23) Watanabe, Y.; Takahashi, S.; Ito, S.; Tokiwa, T.; Noguchi, Y.; Azami, H.; Kojima, H.; Higo, M.; Ban, S.; Nagai, K.; Hirose, T.; Sunazuka, T.; Yaguchi, T.; Nonaka, K.; Iwatsuki, M. Hakuhybotrol, a Polyketide Produced by Hypomyces Pseudocorticiicola, Characterized with the Assistance of 3D ED/MicroED. *Org. Biomol. Chem.* **2023**, *21* (11), 2320–2330.

(24) Xue, D.; Xu, M.; Madden, M. D.; Lian, X.; Older, E. A.; Pulliam, C.; Hui, Y.; Shang, Z.; Gupta, G.; Raja, M. K.; Wang, Y.; Sardi, A.; Long, Y.; Chen, H.; Fan, D.; Bugni, T. S.; Testerman, T. L.; Wu, Q.; Li, J. Discovery of A Chimeric Polyketide Family as Cancer Immunogenic Chemotherapeutic Leads. *bioRxiv*, **2024**.

(25) Curtis, B. J.; Kim, L. J.; Wrobel, C. J. J.; Eagan, J. M.; Smith, R. A.; Burch, J. E.; Le, H. H.; Artyukhin, A. B.; Nelson, H. M.; Schroeder, F. C. Identification of Uric Acid Gluconucleoside-Ascaroside Conjugates in Caenorhabditis Elegans by Combining Synthesis and MicroED. *Org. Lett.* **2020**, *22* (17), 6724–6728.

(26) Kim, L. J.; Xue, M.; Li, X.; Xu, Z.; Paulson, E.; Mercado, B.; Nelson, H. M.; Herzon, S. B. Structure Revision of the Lomaiviticins. *J. Am. Chem. Soc.* **2021**, *143* (17), 6578–6585.

(27) Kim, L. J.; Ohashi, M.; Zhang, Z.; Tan, D.; Asay, M.; Cascio, D.; Rodriguez, J. A.; Tang, Y.; Nelson, H. M. Prospecting for Natural Products by Genome Mining and Microcrystal Electron Diffraction. *Nat. Chem. Biol.* **2021**, *17* (8), 872–877.

(28) Go, E. B.; Kim, L. J.; Nelson, H. M.; Ohashi, M.; Tang, Y. Biosynthesis of the Fusarium Mycotoxin (-)-Sambutoxin. *Org. Lett.* **2021**, *23* (20), 7819–7823.

(29) Khatri Chhetri, B.; Mojib, N.; Moore, S. G.; Delgadillo, D. A.; Burch, J. E.; Barrett, N. H.; Gaul, D. A.; Marquez, L.; Soapi, K.; Nelson, H. M.; Quave, C. L.; Kubanek, J. Cryptic Chemical Variation in a Marine Red Alga as Revealed by Nontargeted Metabolomics. *ACS Omega* **2023**, *8* (15), 13899–13910.

(30) Lin, S.-Y.; Oakley, C. E.; Jenkinson, C. B.; Chiang, Y.-M.; Lee, C.-K.; Jones, C. G.; Seidler, P. M.; Nelson, H. M.; Todd, R. B.; Wang, C. C. C.; Oakley, B. R. A Heterologous Expression Platform in Aspergillus Nidulans for the Elucidation of Cryptic Secondary Metabolism Biosynthetic Gene Clusters: Discovery of the Aspergillus Fumigatus Sartorypyrone Biosynthetic Pathway. *Chem. Sci.* **2023**, *14* (40), 11022–11032.

(31) Yan, C.; Han, W.; Zhou, Q.; Niwa, K.; Tang, M. J.; Burch, J. E.; Zhang, Y.; Delgadillo, D. A.; Sun, Z.; Wu, Z.; Jacobsen, S. E.; Nelson, H.; Houk, K. N.; Tang, Y. Genome Mining from Agriculturally Relevant Fungi Led to a D-Glucose Esterified Polyketide with a Terpene-like Core Structure. *J. Am. Chem. Soc.* **2023**, *145* (46), 25080–25085.

(32) Abad, A. N. D.; Seshadri, K.; Ohashi, M.; Delgadillo, D. A.; de Moraes, L. S.; Nagasawa, K. K.; Liu, M.; Johnson, S.; Nelson, H. M.; Tang, Y. Discovery and Characterization of Pyridoxal 5'-Phosphate-Dependent Cycloleucine Synthases. *J. Am. Chem. Soc.* **2024**, *146* (21), 14672–14684.

(33) Powell, S.; Herrera, D.; El Khoury, I.; Perdue, C.; Sadler, N.; Cort, J.; Robinson, G.; Handakumbura, P.; Evans, J.; Lin, V. *Accelerating the Identification of Novel Secondary Metabolites in Bioenergy Plant Root Exudates Using MicroED*; Office of Scientific and Technical Information (OSTI), **2024**.

(34) Grkovic, T.; Akee, R. K.; Thornburg, C. C.; Trinh, S. K.; Britt, J. R.; Harris, M. J.; Evans, J. R.; Kang, U.; Ensel, S.; Henrich, C. J.; Gustafson, K. R.; Schneider, J. P.; O'Keefe, B. R. National Cancer Institute (NCI) Program for Natural Products Discovery: Rapid Isolation and Identification of Biologically Active Natural Products from the NCI Prefractionated Library. *ACS Chem. Biol.* **2020**, *15* (4), 1104–1114.

(35) Martínez-Fructuoso, L.; Arends, S. J. R.; Freire, V. F.; Evans, J. R.; DeVries, S.; Peyser, B. D.; Akee, R. K.; Thornburg, C. C.; Kumar, R.; Ensel, S.; Morgan, G. M.; McConachie, G. D.; Veeder, N.; Duncan, L. R.; Grkovic, T.; O'Keefe, B. R. Screen for New Antimicrobial Natural Products from the NCI Program for Natural Product Discovery Prefractionated Extract Library. *ACS Infect. Dis.* **2023**, *9* (6), 1245–1256.

(36) Delgadillo, D. A.; Burch, J. E.; Kim, L. J.; de Moraes, L. S.; Niwa, K.; Williams, J.; Tang, M. J.; Lavallo, V. G.; Khatri Chhetri, B.; Jones, C. G.; Rodriguez, I. H.; Signore, J. A.; Marquez, L.; Bhanushali, R.; Woo, S.; Kubanek, J.; Quave, C.; Tang, Y.; Nelson, H. M. High-Throughput Identification of Crystalline Natural Products from Crude Extracts Enabled by Microarray Technology and MicroED. *ACS Cent. Sci.* **2024**, *10* (1), 176–183.

(37) theNelsonLab. *AutoProcess*. GitHub. https://github.com/theNelsonLab.

(38) Saha, A.; Nia, S. S.; Rodríguez, J. A. Electron Diffraction of 3D Molecular Crystals. *Chem. Rev.* **2022**, *122* (17), 13883–13914.

(39) Bailly, C. Naming of New Natural Products: Standard, Pitfalls and Tips-and-Tricks. *Phytochemistry* **2022**, *200* (113250), 113250.

(40) Huu Tai, B.; Xuan Nhiem, N.; Hai Yen, P.; Hong Quang, T.; Thi Cuc, N.; Thi Trang, D.; Van Doan, V.; Thuy Hang, D. T.; Van Minh, C.; Van Kiem, P. Three New Muurolane-Type Sesquiterpene Glycosides from the Whole Plants of Balanophora Fungosa Subsp. Indica. *Nat. Prod. Res.* **2020**, *34* (20), 2964–2970.

(41) Greco, C.; Pfannenstiel, B. T.; Liu, J. C.; Keller, N. P. Depsipeptide Aspergillicins Revealed by Chromatin Reader Protein Deletion. *ACS Chem. Biol.* **2019**, *14* (6), 1121–1128.

(42) Holzapfel, C. W. The Isolation and Structure of Cyclopiazonic Acid, a Toxic Metabolite of Penicillium Cyclopium Westling. *Tetrahedron* **1968**, *24* (5), 2101–2119.

(43) Saetang, P.; Rukachaisirikul, V.; Phongpaichit, S.; Preedanon, S.; Sakayaroj, J.; Hadsadee, S.; Jungsuttiwong, S. Aspertamarinolides A-C: γ-Butenolides from the Marine-Derived Fungus Aspergillus Tamarii PSU-MF90. *Tetrahedron Lett.* **2020**, *61* (46), 152529.

(44) Leman-Loubière, C.; Le Goff, G.; Retailleau, P.; Debitus, C.; Ouazzani, J. Sporothriolide-Related Compounds from the Fungus Hypoxylon Monticulosum CLL-205 Isolated from a Sphaerocladina Sponge from the Tahiti Coast. *J. Nat. Prod.* **2017**, *80* (10), 2850–2854.

(45) Cao, L.; Yan, W.; Gu, C.; Wang, Z.; Zhao, S.; Kang, S.; Khan, B.; Zhu, H.; Li, J.; Ye, Y. New Alkylitaconic Acid Derivatives from Nodulisporium Sp. A21 and Their Auxin Herbicidal Activities on Weed Seeds. *J. Agric. Food Chem.* **2019**, *67* (10), 2811–2817.